Multiaxial magnetic ordering in NdMg

1998 J. Phys.: Condens. Matter 10 165

(http://iopscience.iop.org/0953-8984/10/1/018)

J. Phys.: Condens. Matter **10** (1998) 165–174. Printed in the UK PII: S0953-8984(98)87197-X

Multiaxial magnetic ordering in NdMg

M Deldem†, M Amara†, R M Galéra†, P Morin†, D Schmitt† and B Ouladdiaf‡

† Laboratoire Louis-Néel§, CNRS, BP 166X, 38042 Grenoble Cédex 9, France
‡ Institut Laue–Langevin, BP 156, 38042 Grenoble Cédex 9, France

Received 27 August 1997, in final form 15 October 1997

Abstract. NdMg is a cubic compound (CsCl-type) which orders antiferromagnetically at $T_N = 61$ K. The magnetization measurements show a second transition at $T_R = 35$ K. Over the whole order range, the powder neutron diffraction pattern can be indexed on the hypothesis of a collinear structure, the magnetic moments being parallel to the $\langle \frac{1}{2}\,0\,0 \rangle$ wave vector. The neutron diffraction experiments on a single crystal, under an applied magnetic field, establish that the transition at T_R corresponds to a change from a collinear structure to a multiaxial one. The magnetic moments successively point along a fourfold axis, in the collinear structure, and along twofold axes in the multiaxial one. This sequence of magnetic structures is consistent with the coexistence of ferroquadrupolar γ-couplings and antiferroquadrupolar ε-couplings.

1. Introduction

Rare-earth intermetallic compounds present a large variety of antiferromagnetic structures, which result from the coexistence of various two-ion and one-ion interactions [1]. For lattices in which the rare-earth ions are at sites possessing multiple n-fold symmetry axes, the magnetic order ground state would be degenerate if just the crystal-field anisotropy and the RKKY bilinear interactions were considered. The actual magnetic structure is determined by high-order pair interactions. The predominant ones are established as being of quadrupolar type in, at least, the cubic rare-earth compounds RAg, RCu, RCd and RZn, which have the CsCl-type structure [2]. Although these couplings are in most cases dominated by the bilinear ones, they remain active in selecting the most energetically favourable magnetic structure [3]. Ferroquadrupolar interaction for the Γ_3 quadrupolar representation (FQ γ) and ferroquadrupolar interaction for the Γ_5 representation (FQ ε) lead to collinear arrangements for the quadrupolar moments, then for the magnetic ones. Antiferroquadrupolar interactions determine, from site to site, a different direction among a given crystallographic set, i.e. a multiaxial structure. The proof of the existence of such a structure may be achieved by means of neutron scattering on a single crystal, under an applied magnetic field [4]. Another experimental probe appropriate for use in investigating a multiaxial structure would consist in the x-ray diffraction associated with the periodical orientation of the 4f aspherical shell. Looking for a rare-earth compound well adapted for x-ray diffraction experiments, we have undertaken the study of the NdMg compound. Indeed, this compound crystallizes within the CsCl-type cubic structure and has a favourable behaviour as regards oxidization. From powder neutron diffraction experiments at 4.2 K,

§ Associated with the Joseph Fourier University of Grenoble.

0953-8984/98/010165+10$19.50

NdMg is reported as an antiferromagnet [5], the propagated moment (on the hypothesis of a collinear structure) being parallel to the $\langle \frac{1}{2}\,0\,0 \rangle$ wave vector. In addition to the collinear one, such a pattern is compatible with two multiaxial magnetic structures [6]. NdMg is then very reminiscent of NdZn [7], unfortunately excessively oxidizable. In order to check the existence of multiaxial magnetic ordering in NdMg, we have investigated its ordered range by means of magnetization (section 2) and neutron diffraction measurements (section 3). As results, the low-field magnetic phase diagrams are obtained and the spontaneous magnetic structures unambiguously determined.

2. Magnetization measurements

The magnetization measurements have been performed at the Laboratoire Louis-Néel by the extraction method in magnetic fields up to 11 T. The temperature range of the measurements extends from 1.5 K to room temperature. The single-crystalline sphere used was cut from an ingot prepared by the Bridgman technique in a sealed tantalum crucible. Isothermal and isofield measurements have been carried out for the three main crystallographic directions. Isothermal magnetization curves were used for extracting the magnetic susceptibilities and, also, for locating transition lines on the (H, T) phase diagram. Isofield measurements were also performed, because they are well suited for locating nearly vertical transition lines on the magnetic phase diagrams.

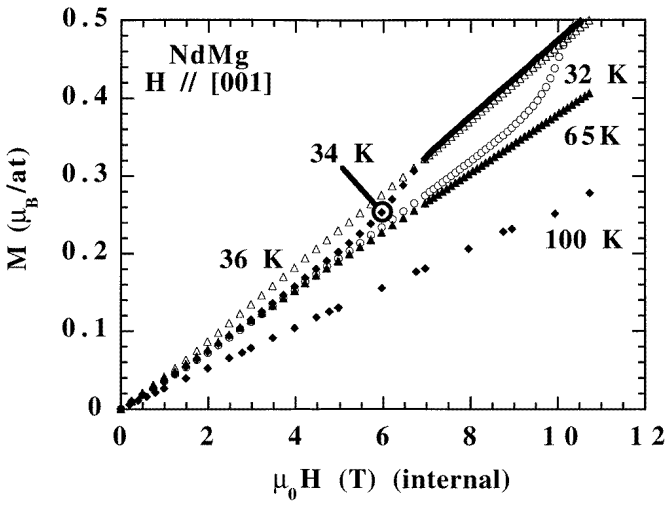

Figure 1. Isothermal magnetization measurements on NdMg for a magnetic field applied along the [0 0 1] direction at $T = 32$, 34, 36, 65 and 100 K. The field values are corrected for the demagnetizing effects.

2.1. Magnetic first-order susceptibility

The first-order magnetic susceptibility has been derived, using Arrott plots, from the isothermal magnetization measurements for the fourfold direction of the applied magnetic field. Figure 1 shows some isothermal magnetization curves obtained for this field direction. In the paramagnetic range, the $M(H)$ curves appear fairly linear up to the maximum field, the same being observed for the twofold and threefold field directions. From Arrott plots, the

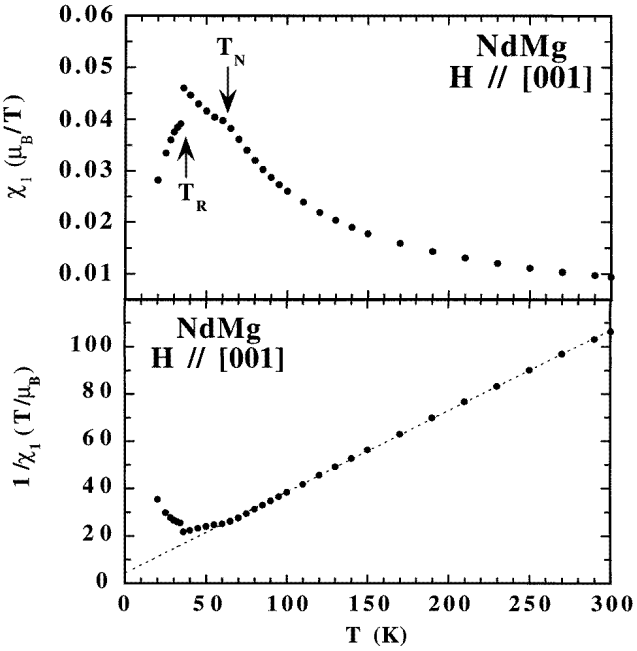

Figure 2. Upper part: the magnetic susceptibility of NdMg as derived from Arrott plots for a field applied along a fourfold axis. Lower part: the reciprocal magnetic susceptibility of NdMg. Above T_N, a linear fit (dotted line) to the experimental curve is rather satisfactory, with a bilinear coupling constant θ^* of about -12 K.

third-order susceptibility is weakly negative, with absolute values of order 10^{-5} μ_B T^{-3}. With a maximum applied field of 11 T, the measurements are not accurate enough for defining a clear trend within the paramagnetic range. This is a common observation for antiferromagnetic systems exhibiting a high Néel temperature and a negative Curie–Weiss coupling constant. The lower part of figure 2 shows the reciprocal first-order susceptibility versus the temperature in the 1.5–300 K range. The curve shows no crystal-electric-field deviation from the Curie–Weiss law. In the paramagnetic range, the slope is in tight agreement with the Curie constant of the $J = 9/2$ Hund's rules ground-state multiplet of Nd^{3+}. The Curie–Weiss coupling constant θ^* is negative, of order -12 K. For the fourfold direction of the applied magnetic field, the magnetic order temperature coincides not with a maximum of the $\chi_1(T)$ susceptibility (figure 2, upper part), but with a change of slope occurring slightly above 60 K. A second transition is revealed as a sharp decrease of the susceptibility at 35 K. Two types of magnetic ordering do then spontaneously stabilize in NdMg, the first one below T_N and the second one below a temperature which will be referred to as T_R in the following.

2.2. Magnetic phase diagrams

Using the isofield magnetization measurements, the (H, T) phase diagrams for applied fields up to $\mu_0 H = 11$ T have been derived for the three field directions. As shown in figure 3, these isofield curves are very similar for the different field directions. In particular, in the paramagnetic range, the $M(T)$ curves are superimposable, as the first-order susceptibility

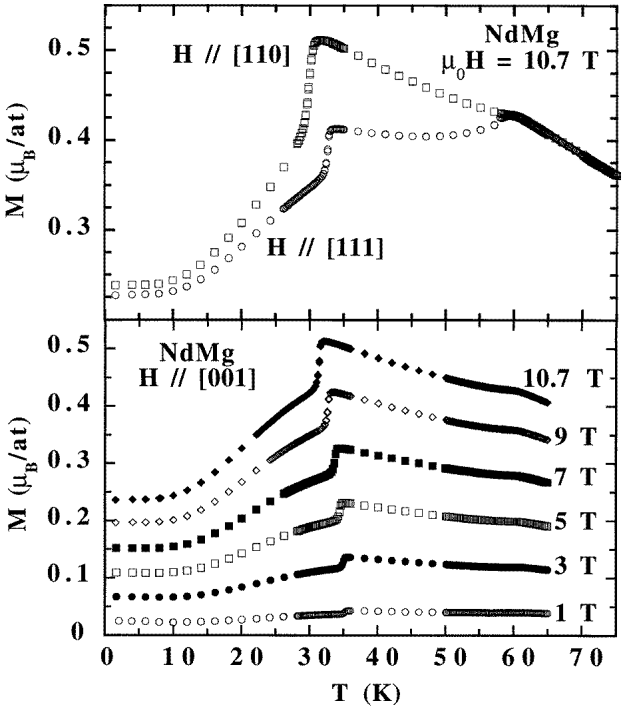

Figure 3. Upper part: isofield magnetization measurements on NdMg for a 10.7 T field applied along twofold and threefold axes. Lower part: a set of isofield magnetization curves measured for a magnetic field along a fourfold direction.

curves for a cubic system should be. This is not surprising if one considers that the $M(H)$ curves are linear up to the maximum field value. Below the order temperature, the $M(T)$ curves do separate, particularly in the high-temperature phase where the system appears more susceptible along a fourfold or twofold direction than along a threefold one.

In the following, we focus on the fourfold direction of the applied magnetic field (the lower part of figure 3). The magnetization step corresponding to T_R and the magnetic order temperature are easily located at any field value. Extrapolating to zero field, these anomalies confirm that $T_R = 35$ K and give a more accurate determination for $T_N = 61$ K. Isothermal magnetization measurements show no noticeable anomalies except for temperatures slightly below T_R (figure 1). For instance, at $T = 34$ K, a small magnetization jump is observed for $\mu_0 H$ around 7 T, in agreement with the $\mu_0 H = 7$ T isofield curve anomaly. Above and below the critical field, the magnetization versus the internal field may be extrapolated to zero in zero field, which demonstrates that the two successive phases are both antiferromagnetic. This explains the regular increase of the magnetization jump with the field on the isofield curves, which is a direct consequence of the susceptibility difference between the two phases. As the field increases, the low-temperature phase having a lower magnetic susceptibility gives way to the high-temperature phase. This results in the slight curvature toward the field axis of the transition line starting from T_R in zero field. No field-induced phases are evident and the phase diagrams display only the two spontaneous magnetic phases for the three field directions. In the following, these two phases will be referred to as I and II, according to the phase diagram plot of figure 4.

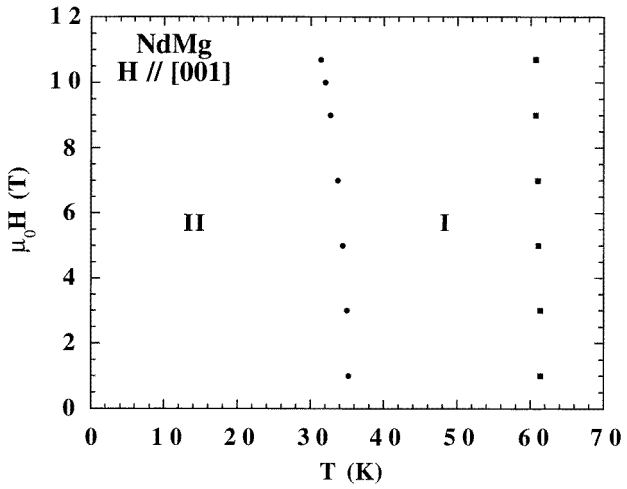

Figure 4. The magnetic phase diagram of NdMg for a magnetic field applied along a fourfold axis. At these levels of magnetic field, the phase diagrams for the three field directions are almost superimposable. The two spontaneous phases are labelled I and II.

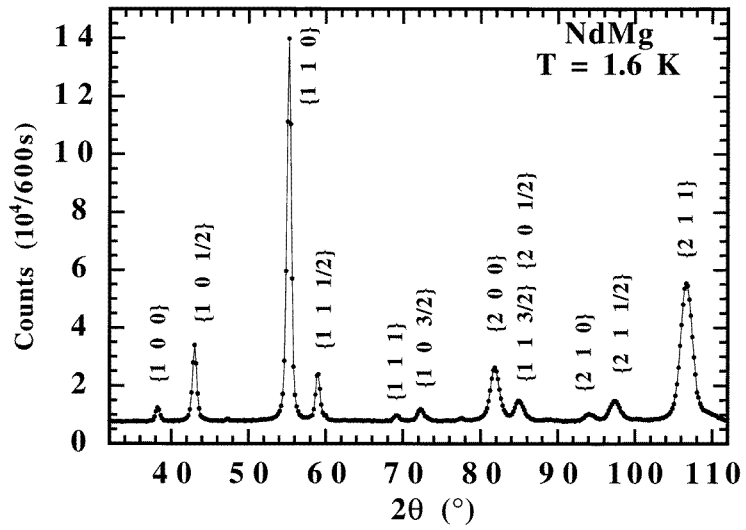

Figure 5. The neutron powder diffraction pattern of NdMg for $T = 1.6$ K.

3. Neutron diffraction experiments

3.1. Powder neutron diffraction

In order to determine the magnetic structures associated with the spontaneous phases I and II, part of a polycrystalline ingot of NdMg has been powdered. First tests using an x-ray Debye–Scherrer diffractometer have attested to the single-phase character of the sample and the negligible presence of neodymium oxide. In agreement with the literature, the lattice parameter is found to be equal to 3.87 Å at room temperature.

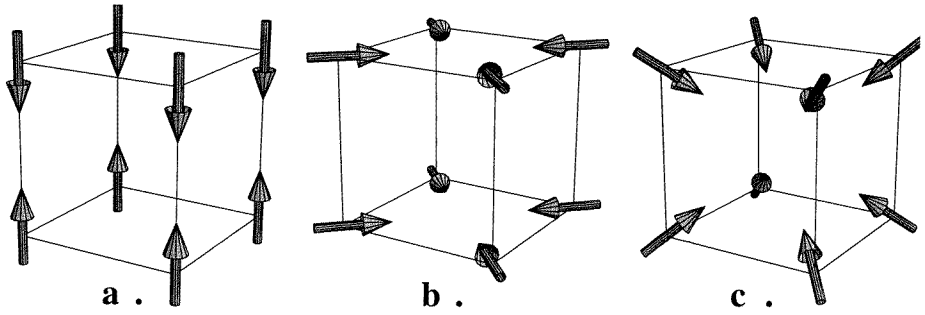

Figure 6. Magnetic structures compatible with the powder neutron diffraction results of NdMg: (a) single-$\boldsymbol{k}$, (b) double-$\boldsymbol{k}$, (c) triple-$\boldsymbol{k}$ structure.

The powder diffraction experiment was carried out on the D1B diffractometer at the ILL. The cryostat used allows for temperatures from 1.5 to 300 K. The powder was installed inside a cylindrical vanadium container, the exposed volume being approximately five cubic centimetres. The neutron wavelength was set at 2.523 Å. The 400-cell multidetector was first positioned in order to cover the 16–96° two-theta angle range. While cooling the sample, the spectra could then include the two-theta position of the $\{\frac{1}{2}\,0\,0\}$ magnetic reflections for which the counts did not exceed the background level. This is in agreement with the low-temperature results of Buschow *et al* [5] and attests to the parallelism of the magnetic moments and the wave vector in the case of a collinear structure. As the $\{\frac{1}{2}\,0\,0\}$ magnetic reflections are zero over the total temperature range, the two-theta angle range was then set to 32–112°, giving access to additional magnetic and nuclear reflections. Thereafter, the patterns were collected while increasing the temperature step by step from 1.5 to 70 K. Figure 5 shows one of the indexed patterns. The peak intensities, corrected for the Lorentz factor, were derived from the raw data using the ABFfit integrating software [8], assuming pseudo-Lorentzian peak profiles.

Within the collinear hypothesis, all of the data collected were analysed, taking the structure as single-$\boldsymbol{k}$ $\langle\frac{1}{2}\,0\,0\rangle$, with the Fourier component parallel with the wave vector. This has required the magnetic theoretical intensities to be computed using the relation

$$I_{\mathrm{calc}}(2\theta) = C_{\mathrm{app}} \sum_{\substack{\boldsymbol{Q} \\ |\boldsymbol{Q}|=\mathrm{cst}}} (C_{\mathrm{magn}} f(\sin\theta/\lambda) \boldsymbol{M}_{\boldsymbol{k}} \sin(\boldsymbol{Q}, \boldsymbol{M}_{\boldsymbol{k}}))^2$$

where C_{app} is the apparatus constant (determined from the nuclear reflections), $C_{\mathrm{magn}} \approx 0.569 \times 10^{-12}$ cm is the magnetic diffusion constant, $f(\sin\theta/\lambda)$ is the magnetic form factor [9] and $\boldsymbol{M}_{\boldsymbol{k}}$ is the single magnetic Fourier component with wave vector $\boldsymbol{k}$. The summation is carried over all of the $\boldsymbol{Q}$ scattering vectors from the Ewald sphere associated with a given two-theta angle, $(\boldsymbol{k}, \boldsymbol{M}_{\boldsymbol{k}})$ being fixed. Obviously, only scattering vectors $\boldsymbol{Q}$ such that $\boldsymbol{Q} + \boldsymbol{k} = \boldsymbol{H}$, where $\boldsymbol{H}$ belongs to the reciprocal crystallographic lattice, will make a non-zero contribution to the magnetic reflections. Table 1 gives the detail of the adjustment between the experimental and calculated intensities at $T = 1.6$ K. The deduced amplitude of the magnetic moment reaches $2.56 \pm 0.1\ \mu_B$ at this lowest temperature.

In addition to this single-$\boldsymbol{k}$ model, a double-$\boldsymbol{k}$ model, with moments along twofold axes, and a triple-$\boldsymbol{k}$ model, with moments along threefold axes, may also be considered [6, 10]. These three structures, compatible with the powder neutron diffraction results, are represented in figure 6.

Table 1. Experimental and computed powder diffraction intensities for $T = 1.6$ K. The intensities are computed using a 2.56 μ_B amplitude for the ordered moment. The discrepancy observed for the $\{1\,0\,\frac{3}{2}\}$ reflections originates from an imperfect integration due to a close parasitic peak.

	$\{1\,0\,\frac{1}{2}\}$	$\{1\,1\,\frac{1}{2}\}$	$\{1\,0\,\frac{3}{2}\}$	$\{1\,1\,\frac{3}{2}\}, \{2\,0\,\frac{1}{2}\}$	$\{2\,1\,\frac{1}{2}\}$
I_{measured}	5094	5704	2349	7687	10 049
$I_{\text{calculated}}$	5446	5648	1793	2528, 5054	9486
Error (%)	6.91	0.98	23.7	1.36	5.60

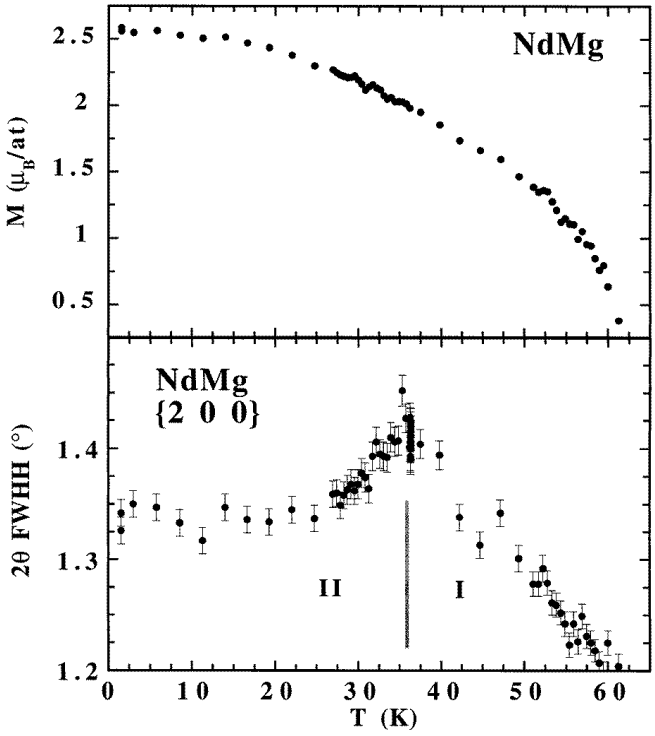

Figure 7. Upper part: the thermal evolution of the ordered moment of NdMg as deduced from the powder neutron diffraction measurements. Lower part: the thermal evolution of the full width at half-height for the {2 0 0} nuclear reflections.

Crossing the transition temperature T_R, no discontinuity is observed in the magnetic moment amplitude (figure 7, upper part). However, if one considers the thermal evolution of the width of the nuclear peaks, some effect may be noticed around T_R, such as the broadening of the {2 0 0} reflections above 35 K (figure 7, lower part). This is however difficult to relate to a particular sequence of magnetic structures. In addition, although the data have been analysed on the basis of commensurate $\langle \frac{1}{2}\,0\,0 \rangle$ wave vectors, one cannot exclude the hypothesis of a small modulation which could have not been revealed within the experimental resolution. To resolve these uncertainties, the powder diffraction results need to be completed by means of a neutron diffraction experiment on a single crystal.

3.2. Single-crystal neutron diffraction

The neutron diffraction experiments were carried out at the ILL, on the S20 diffractometer (double axis, with a moving-up counter). On this instrument, the cryomagnet can provide magnetic fields up to $\mu_0 H = 6$ T in the 1.5–300 K temperature range. The sample used, of the same origin as the sphere used for magnetization measurements, has a roughly parallelepipedic shape ($4 \times 4 \times 12$ mm^3). This crystal was lined up with a twofold axis parallel with the vertical magnetic field direction, which will be referred to as $[1\,{-1}\,0]$.

The aim of this experiment was to resolve the remaining ambiguities as regards the magnetic structures after the powder neutron diffraction measurements. Taking advantage of the higher resolution in the reciprocal space, we first intended to check the absence of any magnetic modulation, i.e. to see whether the magnetic propagation vectors effectively belong to the $\langle \frac{1}{2}\,0\,0 \rangle$ star. This was achieved by carrying out zero-field scans in the reciprocal space around the magnetic reflections associated with the $\langle \frac{1}{2}\,0\,0 \rangle$ star. For instance, for the $[1\,{-0.5}\,0]$ reflection, scans have been done on one index (h or k) and simultaneously on two (h and k) or three indexes. The total range of these scans exceeded by far the resolution width of the powder diffraction experiment. None of these scans have provided evidence for magnetic peaks apart from the $[1\,{-0.5}\,0]$ reflection, and this for temperatures ranging from 10 K up to a maximum of 80 K. Thus, it is highly likely that the only wave vectors involved in the spontaneous structures of NdMg belong to the $\langle \frac{1}{2}\,0\,0 \rangle$ star.

It remains to determine which of the structures retained after the powder diffraction experiments (figure 6) effectively correspond to phases I and II. In view of this determination, let us consider the effect on the domain partition of a magnetic field applied along a twofold axis. For a given structure, the field selects the domains with maximum magnetic susceptibility. In an antiferromagnet, these are the domains for which the magnetic moments are the most nearly perpendicular to the field direction. In the case of a collinear structure with fourfold directions of easy magnetization (figure 6(a)), only the domain with moments perpendicular to the twofold field direction is favoured. Consequently, for this collinear structure, a single branch of the $\langle \frac{1}{2}\,0\,0 \rangle$ star should prevail. For the double-$\boldsymbol{k}$ structure (figure 6(b)), two domains are equivalent with respect to the field and will be selected at the expense of the third one. One branch of the propagation star is simultaneously involved in these two domains, whereas the two others appear in the description of just one domain. This will result in the prevalence of one branch, the two others, however, still being, present. The triple-$\boldsymbol{k}$ magnetic structure (figure 6(c)) preserves the cubic symmetry and thus corresponds to a single domain in which all of the $\langle \frac{1}{2}\,0\,0 \rangle$ branches are present.

In order to test these different behaviours, we have measured, while cooling the sample from 80 K down to 10 K in a 5 T field, the integrated intensities of the reflections associated with the three independent branches of the $\langle \frac{1}{2}\,0\,0 \rangle$ propagation star (figure 8). The value of the magnetic field was chosen for an efficient domain selection without an excessive distortion of the structures, as attested to by the weak susceptibilities displayed by the $M(H)$ curves (figure 1). In the 38–60 K range, one of the reflections, $[{-1}\,{-1}\,0.5]$, amply dominates over the two others ($[{-0.5}\,{-1}\,1]$ and $[{-1}\,{-0.5}\,1]$), which is only compatible with a collinear structure. Thus, among the three structures allowed by the powder neutron diffraction results, the single-$\boldsymbol{k}$ one with moments along fourfold axes is associated with phase I. This is consistent with the magnetization results showing a reduced susceptibility for a field along a threefold direction in comparison with the fourfold or twofold directions. For the threefold direction, the angle between the moments and the field is 54.7°, whereas for the fourfold and twofold directions this angle is 90° (for the favoured domains), which results in an effective transverse response of the moments.

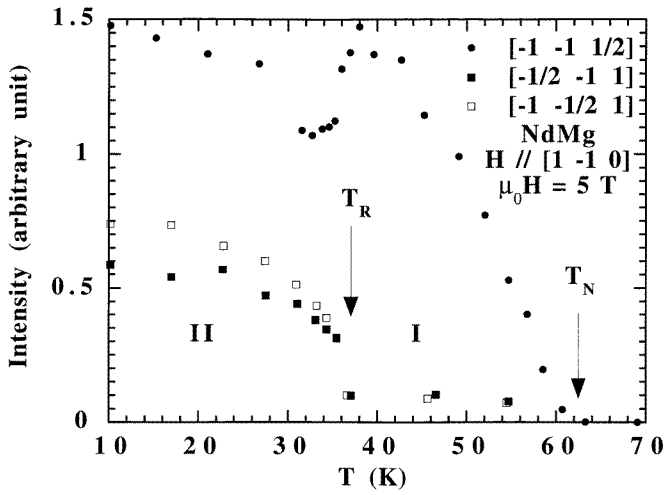

Figure 8. Thermal evolution in a $[1\,{-}1\,0]$ field of 5 T of the intensities of three antiferromagnetic reflections associated with each branch of the $\langle \frac{1}{2}\,0\,0 \rangle$ propagation star.

Entering phase II, the dominant intensity slightly decreases while the two others become no longer negligible, reaching about one half of the $[{-}1\,{-}1\,0.5]$ reflection at 10 K. This is now what is expected in the case of a multiaxial double-$\boldsymbol{k}$ structure. The transition occurring at T_R thus corresponds to the change from a single-$\boldsymbol{k}$ magnetic structure (figure 6(a)) at high temperature to a double-$\boldsymbol{k}$ structure (figure 6(b)) at low temperature.

4. Conclusion

This study establishes that the NdMg compound presents two spontaneous antiferromagnetic phases. Both correspond to a $\langle \frac{1}{2}\,0\,0 \rangle$ magnetic periodicity, the high-temperature structure being collinear (single-$\boldsymbol{k}$) with moments along a fourfold axis and the low-temperature structure being multiaxial (double-$\boldsymbol{k}$) with moments along twofold axes. Let us recall that, in NdZn, the magnetic moments order along threefold axes (triple-$\boldsymbol{k}$ structure) at $T_N = 70$ K and move towards twofold axes at $T_R = 18$ K (double-$\boldsymbol{k}$ structure). Owing to a pronounced anisotropy of the magnetic moment, a jump of the magnetic moment amplitude of order 0.3 μ_B is observed at T_R [11], in correspondence with a clear first-order specific heat anomaly [12]. In the case of NdMg, the transition occurring at T_R does not correspond to a step on the ordered moment curve. At this temperature, the major internal energy term should come from the bilinear interactions and is then proportional to the square of the ordered moment. The absence of a significant step on the ordered moment curve means that the latent heat at T_R should be very small. This also confirms the weak crystal-field anisotropy, the change of easy axis from fourfold to twofold having little influence on the magnetic moment amplitude. However, for an accurate analysis one cannot avoid the determination of the crystal-electric-field scheme: first, for explaining the value of the magnetic moment amplitude at low temperature, in comparison with that of the free Nd^{3+} ion (2.6 μ_B instead of 3.3 μ_B) and second, for identifying the origin of the transition at T_R which may be ascribed to the crystal-field or/and quadrupolar couplings (see references [12] and [13]).

The change from a collinear to a multiaxial structure is by no means in contradiction

with what may be expected in the presence of quadrupolar couplings. If one refers to the results of [3], the structure associated with phase I is purely ferroquadrupolar with magnetic moments along fourfold axes, which implies that the quadrupolar dispersion curve for the γ (Γ_3) representation respects the inequality $K^{\gamma}(\mathbf{0}) > K^{\gamma}(\frac{1}{2}\ \frac{1}{2}\ 0)$.

On the other hand, the multiaxial structure of phase II, identical with the low-temperature structure of NdZn [7], respects the previous condition on the quadrupolar γ-couplings plus an additional one on the ε (Γ_5) quadrupolar dispersion curve: $K^{\varepsilon}(\frac{1}{2}\ \frac{1}{2}\ 0) > K^{\varepsilon}(\mathbf{0})$. There is then no contradiction as soon as one accepts the possibility of an anisotropic quadrupolar coupling resulting in two quadrupolar dispersion curves, $K^{\varepsilon}(\boldsymbol{q})$ and $K^{\gamma}(\boldsymbol{q})$, having rather different profiles. At least in the case of cubic rare-earth metallic compounds, where the quadrupoles mainly couple via the conduction electrons [14], that seems to be the general case rather than the exception. For instance, as a general tendency, $K^{\gamma}(\mathbf{0})$ is positive whereas $K^{\varepsilon}(\mathbf{0})$ is negative [2]. In the particular case of the NdZn compound, very different quadrupolar γ- and ε-couplings are consistent with the observed magnetic phase diagrams [13]. The same is found for the $AuCu_3$-type compound $TbIn_3$ [15], which also presents collinear and multiaxial spontaneous magnetic structures.

Looking back to the original aim of this study, which was to check on the existence of a multiaxial ordering in NdMg, one should be satisfied with the magnetic structure found for phase II. In the plane defined by the moment directions, the double-$\boldsymbol{k}$ structure corresponds to an antiferroquadrupolar arrangement. Taking this plane as (xy), the quadrupolar component involved is P_{xy}, propagated by the $[\frac{1}{2}\ \frac{1}{2}\ 0]$ vector. This double-$\boldsymbol{k}$ structure is then a favourable candidate for the observation of x-ray antiferroquadrupolar diffraction peaks. Such diffraction peaks are expected to be less than 10^{-4} times a crystallographic reflection and their observation requires an excellent signal-to-noise ratio. This condition is difficult to satisfy for most of the rare-earth intermetallic compounds, for which it is extremely delicate to get good quality surfaces clean of oxide. In the case of NdMg, the cleaving of a single crystal produces surfaces, perpendicular to fourfold directions, which display a good resistance to oxidization and, furthermore, give excellent Laüe diffraction patterns. One can then optimistically consider the use of a NdMg sample for validating the x-ray diffraction as a probe for antiferroquadrupolar orderings.

References

[1] Coqblin B 1977 *The Electronic Structure of Rare-earth Metals and Alloys: The Magnetic Heavy Rare Earths* (New York: Academic)

[2] Morin P and Schmitt D 1990 *Ferromagnetic Materials* vol 5, ed K H J Buschow and E P Wohlfarth (Amsterdam: North-Holland) p 1

[3] Amara M and Morin P 1995 *Physica* B **205** 379

[4] Rossat-Mignod J 1986 *Neutron Scattering in Condensed Matter Research* ed K Sköld and D L Price (New York: Academic)

[5] Buschow K H J, de Jong J P, Zandbergen H W and van Laar B 1975 *J. Appl. Phys.* **46** 1352

[6] Morin P and Pierre J 1975 *Phys. Status Solidi* a **30** 549

[7] Amara M, Morin P and Burlet P 1995 *Physica* B **210** 157

[8] Filhol A, Blanc J Y, Antoniadis A and Berruyer J 1988 *ABFfit for the Vax* ILL manual

[9] Stassis C, Deckman H W, Harmon B N, Desclaux J P and Freeman A J 1977 *Phys. Rev.* B **15** 369

[10] Wintemberger M and Chamard-Bois R 1972 *Acta Crystallogr.* A **28** 341

[11] Fujii H, Uwatoko Y, Motoya K, Ito Y and Okamoto T 1987 *J. Magn. Magn. Mater.* **63–64** 114

[12] Morin P and de Combarieu A 1975 *Solid State Commun.* **17** 975

[13] Amara M and Morin P 1996 *Physica* B **222** 61

[14] Levy P M, Morin P and Schmitt D 1979 *Phys. Rev. Lett.* **42** 1417

[15] Galéra R M, Amara M, Morin P and Burlet P, unpublished